3D Surface Matching and Recognition Using Conformal Geometry

Sen Wang, Yang Wang, Miao Jin, Xianfeng Gu, Dimitris Samaras
State University of New York at Stony Brook
Computer Science Department
Stony Brook, NY 11794, USA
{swang, yangwang, mjin, gu, samaras}@cs.sunysb.edu

Abstract

3D surface matching is a fundamental issue in computer vision with many applications such as shape registration, 3D object recognition and classification. However, surface matching with noise, occlusion and clutter is a challenging problem. In this paper, we analyze a family of conformal geometric maps including harmonic maps, conformal maps and least squares conformal maps with regards to 3D surface matching. As a result, we propose a novel and computationally efficient surface matching framework by using least squares conformal maps. According to conformal geometry theory, each 3D surface with disk topology can be mapped to a 2D domain through a global optimization and the resulting map is a diffeomorphism, i.e., one-to-one and onto. This allows us to simplify the 3D surface-matching problem to a 2D image-matching problem, by comparing the resulting 2D conformal geometric maps, which are stable, insensitive to resolution changes and robust to occlusion and noise. Therefore, highly accurate and efficient 3D surface matching algorithms can be achieved by using conformal geometric maps. Finally, the performance of conformal geometric maps is evaluated and analyzed comprehensively in 3D surface matching with occlusion, noise and resolution variation. We also provide a series of experiments on real 3D face data that achieve high recognition rates.

1. Introduction

3D shape matching is a fundamental issue in 3D computer vision with many applications, such as shape registration, partial scan alignment, 3D object recognition and classification [2, 31, 24, 13]. As 3D scanning technologies improve, large databases of 3D scans require automated methods for matching. However, matching 3D shapes in noisy and cluttered scenes is a challenging task. Generally, the crux of surface matching is finding good shape representations, allowing us to match two given free-form surfaces by comparing their shape representations.

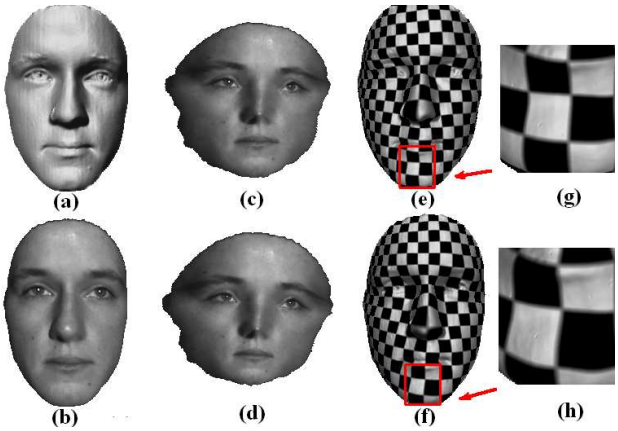

Figure 1. Distortion comparison between a conformal map and a harmonic map. (a) Original surface without texture. (b) Original surface with texture. (c) The 2D conformal map of the surface with texture. (d) The harmonic map of the surface with texture. (e) Checkerbox textured surface by conformal mapping. (f) Checkerbox textured surface by harmonic mapping. Because of angle-preservation, (c) and (e) have less distortions than (d) and (f), which can be clearly seen in the close-up views (g) and (h) of the chin areas in the red boxes respectively.

There has been a lot of research on 3D shape matching in recent decades. The key question in shape matching has been the choice of the shape representation scheme. Different approaches include curvature-based representations[29], regional point representations[16, 24, 28, 3], spherical harmonic representations[17, 8, 9], shape distributions[23] and harmonic shape images[32]. However, many shape representations that use local shape signatures are not stable and cannot perform well in the presence of noise, occlusion and clutter. In this paper, we propose a family of conformal geometric maps that does not suffer from such problems. According to conformal geometry theory, each 3D shape with disk topology can be mapped to a 2D domain through a global optimization and the resulting map is a diffeomorphism, i.e., *one-to-one* and

onto[7, 25, 26, 19]. Consequently the 3D shape-matching problem can be simplified to a 2D image-matching problem of the conformal geometric maps. These maps are stable, insensitive to resolution changes and robust to occlusion and noise. The 2D maps integrate geometric and appearance information and 2D matching is a better understood problem [20, 1, 21]. Therefore, highly accurate and efficient 3D shape matching algorithms can be achieved using conformal geometric maps.

Conformal geometric maps have been used in several applications of computer vision and graphics. In [32], Zhang et al. proposed harmonic maps for surface matching. In [30], Wang et al. use harmonic maps to track dynamic 3D surfaces. In [10], conformal maps are used for face and brain surface matching. Levy et al.[19] use least squares conformal maps for texture atlas generation and Sharon et al.[26] analyze similarities of 2D shapes using conformal maps. However, in order to calculate harmonic maps the surface boundary needs to be identified and a boundary mapping from 3D surfaces to the 2D domain needs to be created, which can be a difficult problem especially when part of the surface is occluded. The two other conformal geometric maps we discuss in this paper, conformal maps and least squares conformal maps, do not need boundary information and so lend themselves as a natural choice to solve this problem. Moreover, in addition to the advantages of harmonic maps, such as sound mathematical basis and preservation of continuity of the underlying surfaces, conformal maps are also angle preserving, which leads to less distortion and robustness to noise. The differences between conformal maps and harmonics maps are shown in Fig. 1.

In this paper, we make the following contributions:

(1) We analyze a family of conformal geometric maps when applied to 3D shape matching and compare their properties comprehensively.

(2) We propose a novel 3D shape matching framework, using least squares conformal maps.

(3) We systematically evaluate the performance of conformal geometric maps on 3D shape matching for different challenges such as occlusion, noise and resolution variation.

(4) We demonstrate conformal geometric maps in practice, through a 3D face recognition application.

The rest of the paper is organized as follows: The mathematical background of the various conformal geometric maps is introduced and compared in Section 2. A framework for 3D shape matching using least squares conformal maps is proposed in Section 3. Experimental results and performance analysis are presented in Section 4, and we conclude with discussion and future work in Section 5.

2. Theoretical background

An important merit of conformal geometric maps, including harmonic maps, conformal maps and least squares conformal maps, is to reduce the 3D shape-matching problem to a 2D image-matching problem, which has been extensively studied[30, 32, 18]. We are dealing with 3D surfaces, but since they are manifolds, they have an inherent 2D structure, which can be exploited to make the problem more tractable using conformal geometry theory[10, 26]. Most work using conformal geometry theory is done in surface parameterization, which can be viewed as an embedding from a 3D surface **S** with disk topology to a planar domain **D**. Following the introduction of the notions of harmonic maps, conformal maps and least squares conformal maps, these three conformal geometric maps will be compared in a comprehensive manner.

2.1. Harmonic maps

As described in [32], a harmonic map $H : S \rightarrow D$ is a critical point for the harmonic energy functional, $E(H) = \int_S \|\nabla H\|^2 d\mu_S$, and can be calculated by minimizing $E(H)$. The norm of the differential $\|\nabla H\|$ is given by the metric on S and D, and μ_S is the area element on 3D surface S[25, 22, 5, 6]. Since the source surface mesh S is in the form of a *discrete* triangular mesh, we approximate the harmonic energy as [5, 32, 10],

$$E(H) = \sum_{[v_0,v_1]} k_{[v_0,v_1]} \|H(v_0) - H(v_1)\|^2, \qquad (1)$$

where $[v_0, v_1]$ is an edge connecting two neighboring vertices v_0 and v_1, and $k_{[v_0,v_1]}$ is defined as

$$\frac{1}{2}\left(\frac{(v_0 - v_2)\cdot(v_1 - v_2)}{\|(v_0 - v_2)\times(v_1 - v_2)\|} + \frac{(v_0 - v_3)\cdot(v_1 - v_3)}{\|(v_0 - v_3)\times(v_1 - v_3)\|}\right)$$

where $\{v_0, v_1, v_2\}$ and $\{v_0, v_1, v_3\}$ are two conjoined triangular faces.

By minimizing the harmonic energy, a harmonic map can be computed using the Euler-Lagrange differential equation for the energy functional, i.e., $\Delta E = 0$, where Δ is the Laplace-Beltrami operator [25, 22, 5, 6]. This will lead to solving a sparse linear least-squares system for the mapping H of each vertex v_i [5, 32, 10]. If the boundary condition $H|_{\partial S} : \partial S \rightarrow \partial D$ is given, the solution exists and is unique.

Although harmonic maps are easy to compute, they require satisfaction of the above boundary condition, which becomes unreliable when there are occlusions in the 3D original data. To overcome this problem, the missing boundaries can be approximated[32], which might be enough for rough surface matching. However, since interior feature points are often more robust to occlusion, it is desirable to replace the boundary condition with feature constraints. This can be achieved by conformal maps, another mathematical tool in conformal geometry theory, which only require several feature constraints as an input and obviate the need to specify the boundary condition.

2.2. Conformal maps

It can be proven that there exists a mapping from any surface with a disk topology to a 2D planar domain[11], which is one-to-one, onto, and angle preserving. This mapping is called *conformal mapping* and keeps the line element unchanged, except for a local scaling factor[7].

Conformal maps have many appealing properties: (1) If the parameterization is conformal, then the surface is uniquely determined (up to a rigid motion) by the mean curvature with area stretching factor defined on the parameter domain. (2) The conformal parameterization can be uniquely determined by 2 corresponding points. (3) Conformal parameterization depends on the geometry itself, not the triangulation of the surfaces. From a practical point of view, conformal parameterization is easy to control. Hence conformal parameterization is crucial for 3D shape matching and recognition.

Consider the case of mapping a planar region S to the plane D. Such a mapping can be viewed as a function of a complex variable, $d = \mathcal{U}(s)$. Locally, a conformal map is simply any function $\mathcal{U}$ which is analytic in the neighborhood of a point s and such that $\mathcal{U}'(s) \neq 0$. A conformal mapping $\mathcal{U}$ thus satisfies the Cauchy-Riemann equations, which are

$$\frac{\partial u}{\partial x} = \frac{\partial v}{\partial y}, \frac{\partial u}{\partial y} = -\frac{\partial v}{\partial x}. \tag{2}$$

where $d = u + iv$ and $s = x + iy$.

Differentiating one of these equations with respect to x and the other with respect to y, we obtain the two Laplace equations

$$\Delta u = 0, \Delta v = 0. \tag{3}$$

where $\Delta = \frac{\partial^2}{\partial x^2} + \frac{\partial^2}{\partial y^2}$. Any mapping which satisfies these two Laplace equations is called a harmonic mapping. Thus a conformal mapping is also harmonic. However, unlike the harmonic maps described in the previous section, which need the boundary mapping $H|_{\partial S}$ fixed in advance, conformal maps can be calculated without demanding the mesh boundary to be mapped onto a fixed shape. For a discrete mesh, the main approaches to achieve conformal parameterizations are: harmonic energy minimization[4, 10], Cauchy-Riemann equation approximation[19], Laplacian operator linearization[11], circle packing[14], most isometric parameterizations(MIPS)[12] and angle-based flattening method[27]. In this paper, we compute conformal maps using the harmonic energy minimization method.

Riemann's theorem states that for any surface S homeomorphic to a disc, it is possible to find a parameterization of the surface satisfying Eq. 2 [19], which can be uniquely determined by two points on surface S. However, to better handle the errors caused by noise in the data and the inaccuracy of finding feature points, we introduce additional feature constraints, indicating that the corresponding features on two 3D surfaces should be mapped onto the same locations in the 2D domain. However, with these additional constraints, it is not always possible to satisfy the conformality condition. Hence, we seek to minimize the violation of Riemann's condition in the least squares sense.

2.3. Least squares conformal maps

The Least Squares Conformal Map(LSCM) parameterization algorithm generates a discrete approximation of a conformal map by adding more constraints. Here we give a brief description (see [19] for details using different constraints).

Given a discrete 3D surface mesh S and a smooth target mapping $\mathcal{U} : S \rightarrow (u, v)$, then, as described in section 2.2, $\mathcal{U}$ is conformal on S if and only if the Cauchy-Riemann equation($\frac{\partial \mathcal{U}}{\partial x} + i\frac{\partial \mathcal{U}}{\partial y} = 0$) holds true on the whole of S. However, in general this conformal condition cannot be strictly satisfied on the whole triangulated surface S, so the conformal map is constructed in the least squares sense:

$$C(S) = \sum_{d \in S} \| \frac{\partial \mathcal{U}}{\partial x} + i\frac{\partial \mathcal{U}}{\partial y} \|^2 A(d) \tag{4}$$

where d is a triangle on the mesh S with the area $A(d)$. Furthermore let $\alpha_j = u_j + iv_j$ and $\beta_j = x_j + iy_j$, so $\alpha_j = \mathcal{U}(\beta_j)$ for $j = 1, 2, ..., n$. Then, we rearrange the vector α such that $\alpha = (\alpha_f, \alpha_p)$ where α_f consists of $n - p$ free coordinates and α_p consists of p constraint point coordinates. Therefore, Eq. 4 can be rewritten as

$$C(S) = \|M_f \alpha_f + M_p \alpha_p\|^2 \tag{5}$$

where $M = (M_f, M_p)$, a sparse $m \times n$ complex matrix. The least squares minimization problem in Eq. 5 can be efficiently solved using the Conjugate Gradient Method. Thus we can map a 3D surface to a 2D domain with multiple correspondences as constraints by using the LSCM technique.

Since LSCMs have almost all the properties of conformal maps and also provide more correspondences as additional constraints, we expect them to be very useful in 3D shape matching and recognition.

2.4. Comparison of conformal geometric maps

Based on conformal geometry theory, harmonic maps, conformal maps and least squares conformal maps(LSCMs) between two topological disks preserve continuity of the underlying surfaces, with minimal stretching energy and angle distortion. All the maps are invariant for the same source surface with different poses, thus making it possible to account for global rigid transformations. A very important property, which governs our matching algorithm, is that all the maps can establish a common 2D parametric domain for

Table 1. Performance comparison of conformal geometric maps.

	Harmonic Maps	Conformal Maps	Least Squares Conformal Maps
Resolution changes	Not sensitive	Not sensitive	Not sensitive
Boundary constraint	Needed	Not needed	Not needed
Boundary occlusion	Difficult to handle	No significant impact	No significant impact
Interior feature points used in mapping	Do not use	Use 2 Points (from Riemann's theorem)	Use more feature constraints
Error of interior feature points detection	Not sensitive	Sensitive	Not sensitive
Computational Complexity	Linear	Nonlinear (with linear approximation available)	Linear

the two surfaces. Therefore we can simplify the 3D shape-matching problem to a 2D image-matching problem. However, they vary in performance for 3D surface matching as can be seen in table 1.

Compared to the exact solutions for harmonic maps and conformal maps, LSCMs are generated by minimizing the violation of Riemann's condition in the least squares sense. This optimization-based parameterization method has the following properties: (1) LSCMs have the same properties as conformal maps, e.g., existence and uniqueness which have already been proven in [19] and preservation of the triangle orientation which means that no triangle flip can occur. (2) LSCMs can map a 3D shape to a 2D domain in a continuous manner with minimized local angle distortion. (3) LSCMs can handle missing boundaries and occlusion and also allow multiple constraints. (4) LSCMs are independent of mesh resolution. (5) The least squares minimization problem in calculating LSCMs has the advantage of being linear.

For actual 3D surfaces, it is very likely to have noise and missing data. From the above comparison, we can see that LSCMs are the best candidate among conformal geometric maps to perform 3D shape matching efficiently. LSCMs do not require the boundary condition explicitly which means they can handle missing boundaries and occlusions. Also, they take multiple feature constraints as input, which allows them to better handle noise introduced by the feature point detection. In the remaining paper, we propose a framework of 3D shape matching using LSCMs.

3. Shape matching framework using least squares conformal maps

To match 3D shapes accurately and efficiently, a new 2D representation, least squares conformal shape images, is developed in our framework using LSCMs. Therefore, we simplify the original 3D shape-matching problem to a 2D image-matching problem. In particular, our shape matching framework includes two steps: First, interior feature correspondences are detected by using spin-images[16]; After that, we generate and match least squares conformal shape images.

3.1. Correspondence detection using spin-images

In order to use least squares conformal mappings, we need to establish interior feature constraints between the 3D shapes. For this purpose, we first select candidate points with curvature larger than a threshold T_c, and then compare their spin-images to detect feature correspondences. The spin-image is a well-known technique that has been proven useful for 3D point matching[16]. It encodes the surface shape surrounding an oriented point p by projecting nearby surface points into a 2D histogram, which has cylindrical coordinates of radius r and height h centered at p, with its axis aligned with the surface normal of p. The number of bins and support size in the spin-image histograms are parameters fixed at generation. It has been shown that the matching results using spin-images are insensitive to the choice of the above parameters [13]. In our experiments, the highest confidence feature correspondences are used. The typical number of selected feature points is 5-6 for 3D face surfaces and 10-12 for brain surfaces.

3.2. Least squares conformal shape images

In this section, we will introduce a method to describe 3D surfaces using least squares conformal shape images (LSCSIs). In section 2.3, we have shown that there exists a least squares conformal mapping that can map each 3D surface with disk topology to the canonical 2D domain. The LSCSIs are generated by associating a shape attribute with each vertex. Mean curvature is a useful geometric attribute that depends only on the surface's geometry. In our method, the mean curvature is computed in the same way as in [10]. Moreover, least squares conformal maps can also help generate additional shape representations by associating other attributes, e.g. texture, which leads to a natural solution of combining multiple important cues for 3D surface matching and recognition, such as shape and texture.

As an example, Fig. 2(d) shows the LSCSI of the surface Fig. 2(b), with higher intensities representing larger mean curvature. Fig. 2(a) is the original surface with texture information and Fig. 2(c) is its LSCM. Fig. 2(e) is the LSCM of a lower resolution(25%) version of the original surface. The similarity between Fig. 2(c) and Fig. 2(e) shows that LSCMs are independent to resolution variation.

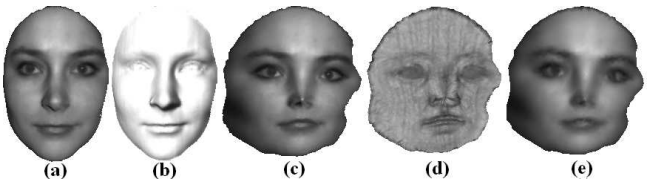

Figure 2. Least Squares Conformal Shape Image: (a) Original surface with texture. (b) Original surface without texture. (c) Least squares conformal maps with texture. (d) Least squares conformal shape image. (e)Least squares conformal maps of the same surface, subsampled by a factor of 4, still very similar to (c).

3.3. Matching surfaces by matching LSCSIs

Given two general surfaces S_1 and S_2 with disk tropology, we first detect high curvature correspondences using spin-images. Then, by incorporating interior correspondences as constraints, LSCSIs are generated for both surfaces as described in section 2.3. After that, the normalized correlation coefficient M_{S_1,S_2} and the similarity criterion $S(S_1, S_2)$ introduced in [15] are computed on the two resulting LSCSIs by

$$M_{S_1,S_2} = \frac{N\sum p_i^{S_1} p_i^{S_2} - \sum p_i^{S_1} \sum p_i^{S_2}}{\sqrt{(N\sum (p_i^{S_1})^2 - (\sum p_i^{S_1})^2)(N\sum (p_i^{S_2})^2 - (\sum p_i^{S_2})^2)}}$$

$$S(S_1, S_2) = (ln\frac{1 + M_{S_1,S_2}}{1 - M_{S_1,S_2}})^2 - \frac{1}{2N} \qquad (6)$$

where N is the number of overlapping points in the LSCSIs of 3D surface S_1 and S_2, and $p_i^{S_k}$ is the value of point i in the LSCSI of surface $S_k (k = 1, 2)$.

However, for 3D surfaces with holes, which violate the disk topology assumption, we can not calculate the LSCMs directly. To overcome this problem, we can simply fill in the holes through interpolation and then use our method to generate the LSCSIs of the new surfaces. As discussed in section 2.4, LSCMs depend on the geometry in a continuous manner, which leads to robustness to local perturbation. Fig. 3 demonstrates the robustness of our method to holes on surfaces. The normalized correlation coefficient of the LSCSIs shown in Fig. 3(b,f) is 0.99, which means a very good match between the two surfaces of Fig. 3(a,e) after hole filling. If we desire to preserve the non-disk topology of the object during matching, then the object should be partitioned into simpler parts with disk topology[19] which could then be matched. Optimal partitioning will be studied in future work.

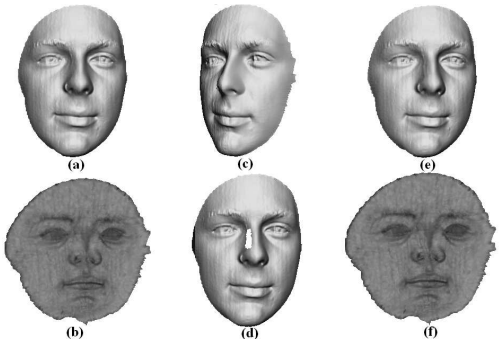

Figure 3. An example of surface matching with holes : (a) A frontal 3D scan. (b) The LSCSI of (a). (c) A side 3D scan of the same subject as in (a), which has a hole illustrated in (d). (e) The same surface of (c,d) after hole filling. (f) The LSCSI of (e).

4. Performance analysis

In this section we analyze the robustness of conformal geometric maps for 3D shape matching with occlusion, noise and resolution variation. We also perform experiments on 3D shape recognition with real data and compare the recognition results of conformal geometric maps with the surface curvature technique of [29].[1]

4.1. Robustness analysis

In this section, we use two surface types: brains (2 instances) and faces (4 instances) to analyze the performance of conformal geometric maps. We present three experiments in which 3D surface matching is performed under occlusion, noise and resolution variation.

4.1.1 Experiments on data occlusion

In this experiment, we test the robustness of conformal geometric maps under occlusion for both face and brain surfaces. Such occlusions might be caused by rotation of the object in front of the scanner. Fig. 4 and 6 show examples of 3D face and brain surfaces respectively, under different occlusions, and the corresponding conformal geometric maps. For each original surface, partially occluded surfaces were generated with occlusion rates between 5% and 45%. Average matching results of these face and brain surfaces using conformal geometric maps are shown in Fig. 5 and 7, respectively. Since the harmonic maps require satisfaction of the surface boundary condition as discussed in section 2.1, the performance of harmonic maps is more impacted than the performance of conformal maps and least squares conformal maps. Instead, changes of boundary have very small effects on both conformal maps and least square conformal maps. In some cases, we superimpose the matched surfaces with significant occlusions (only 60% of area is common

[1] A video of the 3D face matching can be found at: http://www.cs.sunysb.edu/∼ial/expressionModeling.html

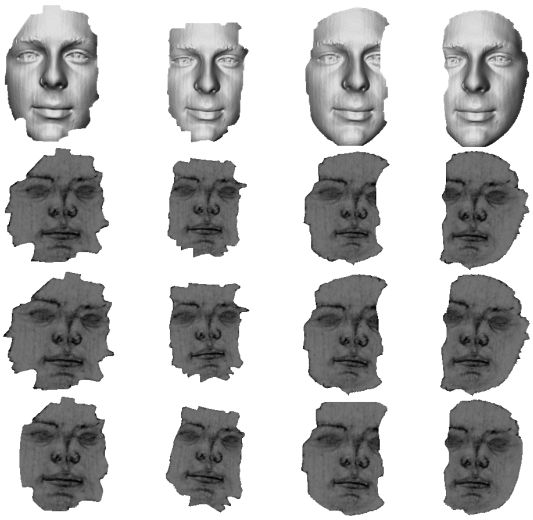

Figure 4. 3D face surfaces and their conformal geometric maps under occlusion. The original 3D face surfaces with different occlusions are in the first row. Their least squares conformal shape images are in the second row. Their conformal maps and harmonic maps with curvature are in the third and the last row, respectively.

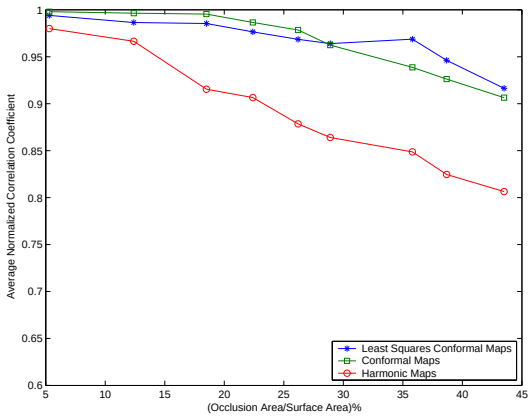

Figure 5. Average matching results of the face surfaces under occlusion.

to both) and the matching error is very hard to detect visually, which suggests that our framework could be useful for partial scan alignment.

4.1.2 Experiments on noisy data

The second experiment tests the robustness of conformal geometric maps in the presence of noise. We add gaussian noise($\mathcal{N}(0,\sigma)$) on each vertex of the face and brain surfaces. σ increases from 0.0 mm to 2.0 mm while the window size for computing the curvatures of 3D face and brain surfaces is 10.5 mm. Example surfaces with noise under two different σ are shown in Fig. 8. We match the various noisy surfaces to the original noise-free surface and the average matching results of the face and brain surfaces are shown in Fig. 9 for various σ values. From the results

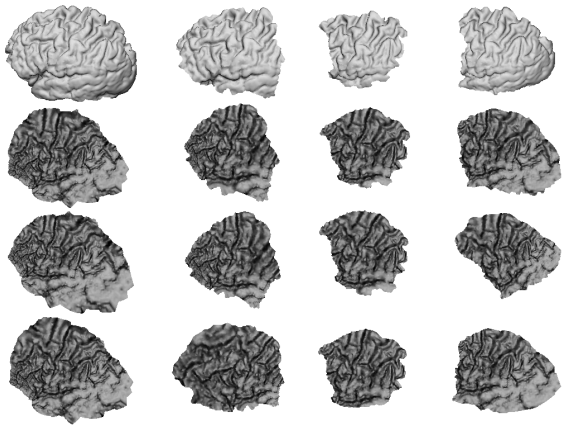

Figure 6. 3D brain surfaces and their conformal geometric maps under occlusion. The original 3D brain surfaces with different occlusions are in the first row. Their least squares conformal shape images are in the second row. Their conformal maps and harmonic maps with curvature are in the third and the last row, respectively.

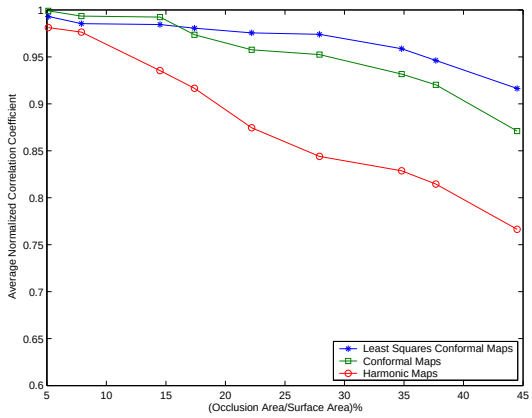

Figure 7. Average matching results of the brain surfaces under occlusion.

we can see that all three conformal geometric maps appear robust to gaussian noise. However, since conformal maps depend on 2 feature points only, which might be detected with errors caused by the noise, they have lower matching rates than the harmonic maps and the least square conformal maps.

4.1.3 Experiments on resolution variation

The third experiment tests the robustness of conformal geometric maps to resolution changes. Fig. 10 shows examples of 3D face and brain surfaces with resolution variation, where all the meshes have the same shape but different resolution. The surfaces with low resolution are matched to the original surfaces and average matching results using the three conformal geometric maps are shown in Fig. 11. Results show that conformal geometric maps achieve fairly stable matching results and all of them are impervious to resolution changes. A small deterioration of the matching

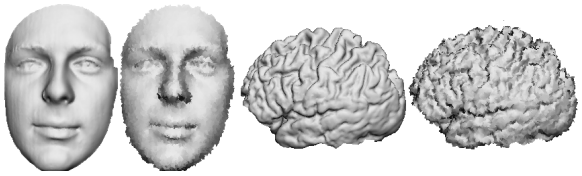

Figure 8. Examples of face and brain surfaces under gaussian noise with different σ set to 0.0 and 2.0 mm, respectively.

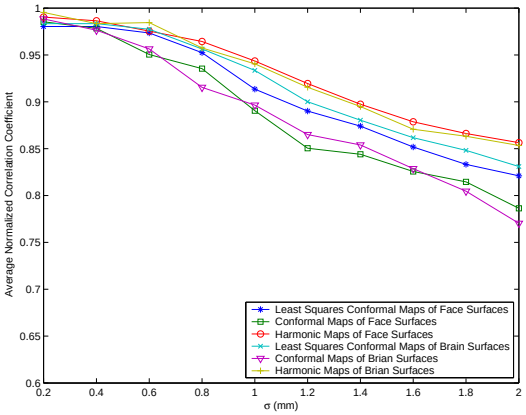

Figure 9. Average matching results of conformal geometric maps under gaussian noise increases. The window size for computing the curvatures of faces surfaces and brain surfaces is 10.5 mm and the σ increases from 0.0 mm to 2.0 mm.

results is due to the use of a discrete curvature approximation, since approximation error increases as the resolution drops.

4.2. Recognition of 3D faces

In this section, we apply conformal geometric maps to 3D face recognition and compare their results with the surface curvature technique of [29]. We use a 3D face database which contains 100 3D face scans from 10 subjects captured by a phase-shifting structured light ranging system. Each face has approximately 80K 3D points with both shape and texture information available (example face data from two subjects in the database are shown in Fig. 12). We perform 3D face recognition using conformal geometric maps and compare them with the surface curvature technique. In each experiment, we randomly select a single face from each subject for the gallery and use all the remaining faces as the probe set. The average recognition results from 20 experiments (with different randomly selected galleries) are reported in Table 2. In this experiment, conformal geometric maps perform 12.3% better than the surface curvature technique even if only the shape information is used. Moreover, conformal geometric maps allow to combine both shape and texture information, which improves the accuracy of 3D face recognition. As we expected, the least squares conformal maps achieve the best recognition result among all three conformal geometric maps.

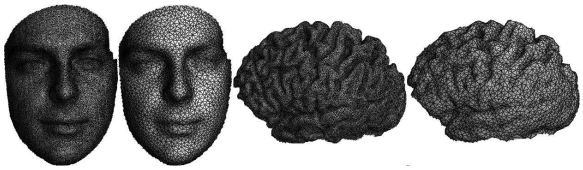

Figure 10. 3D face and brain surfaces with 1 and 1/8 of the original resolution, respectively.

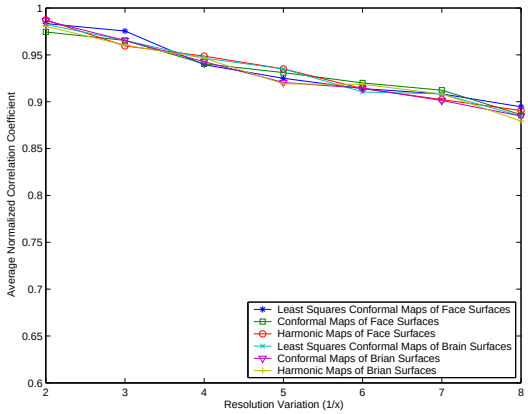

Figure 11. Average matching results of conformal geometric maps under resolution variation.

5. Conclusion and future work

In this paper, we presented a family of conformal geometric maps and proposed a fully automatic and novel 3D shape matching framework using least squares conformal shape images – a new shape representation which simplified the 3D surface-matching problem to a 2D image-matching problem. Furthermore, performance of conformal geometric maps including harmonic maps, conformal maps and least squares conformal maps were systematically evaluated vis-a-vis a surface curvature technique in 3D face recognition. Our results have shown that conformal geometric maps are robust to occlusion, noise and different resolutions and that the least squares conformal mapping is the best choice for 3D surface matching.

In future work, we will continue to exploit the properties of conformal geometric maps and further analyze the properties of conformal geometric shape representations for surfaces with non-disk topology. We will further validate our method as larger databases become available. We plan to use our framework for applications such as 3D object classification and registration under non-rigid deformations.

References

[1] V. Athitsos, J. Alon, S. Sclaroff, and G. Kollios. Boostmap: a method for efficient approximate similarity rankings. In *CVPR04*, pages II: 268–275, 2004.

[2] R. Campbell and P. Flynn. A survey of free-form object representation and recognition techniques. *Computer Vision and Image Understanding*, 81:166–210, 2001.

Table 2. Recognition results of conformal geometric maps and surface curvature technique.

Recognition Result	Harmonic Maps	Conformal Maps	Least Squares Conformal Maps	Surface Curvature
Using shape information only	92.8%	95.7%	97.3%	83.0%
Using texture information only	93.5%	96.5%	98.0%	N/A
Using both shape and texture	93.9%	97.0%	98.4%	N/A

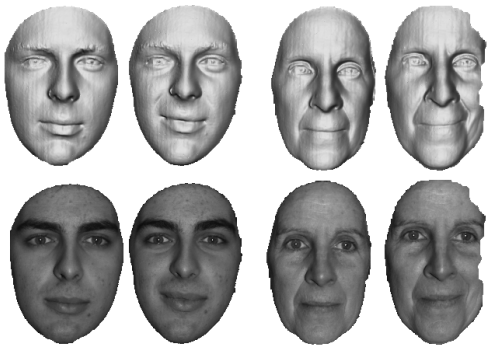

Figure 12. Two subjects in the 3D face database. Shape information is in the first row and texture information is in the second row.

[3] C. Chua and R. Jarvis. 3d free-form surface registration and object recognition. *IJCV*, 17:77–99, 1996.

[4] M. Desbrun, M. Meyer, and P. Alliez. Intrinsic parameterizations of surface meshes. In *Eurographics02*, pages 209–218, 2002.

[5] M. Eck, T. DeRose, T. Duchamp, H. Hoppe, M. Lounsbery, and W. Stuetzle. Multiresolution analysis of arbitrary meshes. In *SIGGRAPH'95*, pages 173–182, 1995.

[6] J. Eells and J. H. Sampson. Harmonic mappings of riemannian manifolds. *Amer. J. Math.*, 86:109–160, 1964.

[7] M. S. Floater and K. Hormann. Surface parameterization: a tutorial and survey. In *Advances in Multiresolution for Geometric Modelling*, pages 157–186. Springer, 2004.

[8] A. Frome, D. Huber, R. Kolluri, T. Bulow, and J. Malik. Recognizing objects in range data using regional point descriptors. In *ECCV04*, May 2004.

[9] T. Funkhouser, P. Min, M. Kazhdan, J. Chen, A. Halderman, D. Dobkin, and D. Jacobs. A search engine for 3d models. In *ACM Transactions on Graphics*, pages 83–105, 2003.

[10] X. Gu, Y. Wang, T. F. Chan, P. M. Thompson, and S. Yaun. Genus zero surface conformal mapping and its application to brain surface mapping. *IEEE Transaction on Medical Imaging*, 23(7), 2004.

[11] S. Haker, S. Angenent, A. Tannenbaum, R. Kikinis, G. Sapiro, and M. Halle. Conformal surface parameterization for texture mapping. *IEEE Transactions on Visualization and Computer Graphics*, 6:181–189, 2000.

[12] K. Hormann and G. Greiner. MIPS: An efficient global parametrization method. In *Curve and Surface Design: Saint-Malo 1999*, pages 153–162. 2000.

[13] D. Huber, A. Kapuria, R. Donamukkala, and M. Hebert. Parts-based 3d object classification. In *CVPR04*, pages II: 82–89, June 2004.

[14] M. Hurdal, K. Stephenson, P. Bowers, D. Sumners, and D. Rottenberg. Coordinate systems for conformal cerebellar flat maps. *NeuroImage*, 11:S467, 2000.

[15] A. Johnson. *Spin-Images: A Representation for 3-D Surface Matching*. PhD thesis, Robotics Institute, CMU, 1997.

[16] A. Johnson and M. Hebert. Using spin images for efficient object recognition in cluttered 3d scenes. *PAMI*, 21:433–449, 1999.

[17] M. Kazhdan, T. Funkhouser, and S. Rusinkiewicz. Rotation invariant spherical harmonic representation of 3d shape descriptors. In *Eurographics/ACM SIGGRAPH symposium on Geometry processing*, pages 156–164, 2003.

[18] V. Kraevoy and A. Sheffer. Cross-parameterization and compatible remeshing of 3d models. In *SIGGRAPH'04*, pages 861–869, 2004.

[19] B. Levy, S. Petitjean, N. Ray, and J. Maillot. Least squares conformal maps for automatic texture atlas generation. In *SIGGRAPH'02*, pages 362–371, 2002.

[20] D. Lowe. Distinctive image features from scale-invariant keypoints. *IJCV*, 60(2):91–110, 2004.

[21] G. Mori, S. Belongie, and J. Malik. Efficient shape matching using shape contexts. *PAMI*, 27(11):1832–1837, 2005.

[22] B. O'Neill. *Elementary Differential Geometry*. 1997.

[23] R. Osada, T. Funkhouser, B. Chazelle, and D. Dobkin. Shape distributions. In *ACM Transactions on Graphics*, volume 21, pages 807–832, 2002.

[24] S. Ruiz-Correa, L. Shapiro, and M. Meila. A new paradigm for recognizing 3-d object shapes from range data. In *ICCV03*, pages 1126–1133, 2003.

[25] R. Schoen and S. T. Yau. *Lectures on Harmonic Maps*. International Press, Harvard Univ., Cambridge MA, 1997.

[26] E. Sharon and D. Mumford. 2d-shape analysis using conformal mapping. In *CVPR04*, pages II: 350–357, 2004.

[27] A. Sheffer and E. de Sturler. Parameterization of faceted surfaces for meshing using angle-based flattening. *Engineering with Computers*, 17(3):326–337, 2001.

[28] Y. Sun and M. Abidi. Surface matching by 3d point's fingerprint. In *ICCV01*, pages II: 263–269, 2001.

[29] B. Vemuri, A. Mitiche, and J. Aggarwal. Curvature-based representation of objects from range data. *Image and Vision Computing*, 4:107–114, 1986.

[30] Y. Wang, M. Gupta, S. Zhang, S. Wang, X. Gu, D. Samaras, and P. Huang. High resolution tracking of non-rigid 3d motion of densely sampled data using harmonic maps. In *ICCV05*, pages I: 388–395, 2005.

[31] J. Wyngaerd, L. Gool, R. Koch, and M. Proesmans. Rotation invariant spherical harmonic representation of 3d shape descriptors. In *ICCV99*, pages 301–306, 1999.

[32] D. Zhang and M. Hebert. Harmonic maps and their applications in surface matching. In *CVPR99*, pages 524–530.